Publ. Astron. Soc. Japan 36, 287–295 (1984)

A 10-GHz Radio Continuum Survey of the Galactic Plane Region. I. A Complex Region at $l=21°$–$26°$

Yoohiaki SOFUE,* Hisashi HIRABAYASHI, Kenji AKABANE
Makoto INOUE, Toshiro HANDA, and Naomasa NAKAI

Nobeyama Radio Observatory, Minamimaki-mura, Minamisaku-gun, Nagano 384-13*

(Received 1983 July 28; accepted 1984 April 6)

Abstract

This is the first of a series of papers presenting results of a 10-GHz radio continuum survey of the galactic plane region using the 45-m telescope at Nobeyama. An extensive study of a complex region at $21°\leq l\leq 26°$, $|b|\leq 1°$ has revealed the following remarkable features.

A Crab-like SNR: Among many supernova remnants detected in the field, the SNR G24.7+0.6 shows an irregular morphology with a filled center and its peak flux spectrum between 5 and 10 GHz is flat. This fact suggests that this object may be a Crab-like SNR.

H II Ring: Two ringlike orientations of H II regions of diameter 50′ and 40′ are found centered on G23.2+0.2 and G24.6+0.0, respectively. They may be physical associations on rings or shells with a diameter of about 100 pc at distances 7 and 9 kpc, respectively. A shock enhanced star formation is suggested for the origin of the rings.

Weak Nonthermal Sources: A comparison with the Bonn 5-GHz survey reveals a number of weak nonthermal sources near the galactic plane. Possible origins of the sources are discussed.

Key words: Galaxy; H II regions; Radio continuum survey; Supernova remnants.

1. Introduction

A number of surveys of the galactic plane region have been made so far at various radio frequencies. Among them the Bonn survey at 5 GHz using the 100-m telescope (Altenhoff et al. 1978) provides maps with the highest angular resolution among the current surveys in the microwave range, revealing a number of interesting features near the galactic plane. A survey with the same angular resolution but at a higher frequency with a filled aperture antenna will certainly provide a powerful means to investigate the physical nature of the objects found in the Bonn survey.

* Nobeyama Radio Observatory, a branch of the Tokyo Astronomical Observatory, University of Tokyo, is a facility open for general use by researchers in the field of astronomy and astrophysics.

† A. von Humboldt Fellow at Max-Planck-Institut für Radioastronomie, Bonn, from June through September, 1983.

For this reason we conducted a survey of the galactic plane region at 10 GHz using the 45-m radio telescope at the Nobeyama Radio Observatory (NRO). The angular resolution of 2′.7 is almost comparable to that of the Bonn survey (2′.6), so that the two surveys can be directly compared. It is known that the galactic radio emission is dominated by nonthermal components at frequencies lower than 5 GHz and by thermal components at higher frequencies (Hirabayashi 1974). The comparison will be therefore particularly useful to discriminate thermal radio sources from nonthermal sources and vice versa.

In this paper we present a map of the 10-GHz total intensity distribution of the region at $l=21°$ to 26°, which contains complexes of H II regions. We compare our results with the Bonn 5-GHz survey and discuss the nature of sources found in the region. A brief report of the results has been given by Sofue et al. (1983). A further report of the whole survey work will be given in a separate paper.

2. Observations

The observations were made in November, 1982 and March and June, 1983. The HPBW of the 45-m antenna was $2'.70\pm0'.03$ at the center frequency of 10.05 GHz. The bandwidth was 500 MHz. We used a cooled parametric amplifier combined with a Dicke-switching system referencing a cooled dummy load at 20-K stage. The system noise temperature was approximately 100 K. We used a circularly polarized feed system and detected one polarization component. The total intensity was obtained by assuming that the circular polarization in sources is negligible. The flux densities and the positions were calibrated using the radio sources 3C48 and 3C348 (Baars et al. 1977; Tabara et al. 1984). The conversion factor between the brightness temperature on the sky and the equivalent flux density per beam area was taken as $T_b/S=0.47\pm0.05$ K Jy^{-1}.

The region at $l=21°$–26° and $b=-1°$ to $+1°$ was mapped by several observations. The scans were made in the direction approximately perpendicular to the galactic plane. Both extreme sides at $b=\pm1°$ of each map were taken to be zero levels. All the maps were combined to get a final map covering the above region. The rms noise on the final map as calculated in an empty small region was about 20 mK in T_b. The data reduction was made using the radioastronomical reduction system at the NRO, a part of which contains the NOD2 reduction package described by Haslam (1974). Scanning effects, which are mainly caused by the weather condition, were removed by using the "pressing" method of Sofue and Reich (1979). The computations were made on a FACOM M200 at NRO.

3. A Complex Region at $21°\leq l\leq26°$

3.1. The Map and Source List

Results of the observations are shown in figure 1 in the form of a contour map of the total surface brightness. The numbers on the contours represent brightness in units of 21.8 mJy/2′.7 beam ($=3.31\times10^{-22}$ W m^{-2} Hz^{-1} sr^{-1} $=10.2$ mK in T_b). We find a large number of discrete sources both compact and extended. Table 1 lists sources with their positions, fluxes, and sizes. The sizes are full widths at half maximum when the source is fitted with a two-dimensional Gaussian brightness distribution using a Gaussian fitting program. Very extended and elongated sources are sometimes not fitted with the program and are not completely picked up. The column entry to the table is explained below:

Column 1: Galactic longitude.

Column 2: Galactic latitude.

Table 1. Source list at 10.05 GHz.

l Δl	b Δb	S_p ΔS_p (Jy/beam)	θ_l $\Delta\theta_l$	θ_b $\Delta\theta_b$	S_t (Jy)	Remark	Date of observation†
21°10′47″	−00°19′04″	0.15	5′.03	4′.06	0.42		83.3
27	29	0.03	1.47	1.16			
21 20 55	−00 37 40	0.81	2.53	2.69	0.80		83.3
11	11	0.03	0.10	0.11			
21 23 06	−00 14 53	0.35	3.0	3.0	0.4		83.3
20	20	0.05	0.5	0.5			
21 27 27	−00 35 01	0.15	2.58	5.87	0.31	Compact H II	83.3
20	12	0.02	0.28	0.80			
21 30 12	−00 52 32	4.58	2.88	2.57	4.65	Crab-like SNR	83.3
11	11	0.12	0.09	0.08			
21 33 19	−00 05 36	0.11	4.08	4.82	0.30		83.3
25	22	0.02	1.18	1.16			
21 37 58	+00 00 02	0.17	2.41	3.55	0.20		83.3
17	15	0.03	0.43	0.62			
21 45 26	−00 01 31	0.12	2.62	2.62	0.11		83.3
20	20	0.03	0.68	0.74			
21 51 13	−00 09 10	0.16	3.85	4.00	0.34	H II	83.3
17	15	0.02	0.59	0.60			
21 52 7	+00 00 47	0.63	2.48	2.72	0.6	Compact H II	83.3
11	11	0.03	0.14	0.15			
21 53 4	−00 21 40	0.29	4.61	4.72	0.87	SNR	83.3
15	17	0.04	0.63	0.79			
21 56 45	+00 05 51	0.13	2.65	2.79	0.13		83.6
17	17	0.03	0.59	0.62			
21 57 28	−00 26 22	0.22	2.31	3.78	0.26	SNR	83.6
24	17	0.05	0.63	0.94			
22 15 7	+00 02 13	0.11	2.32	3.56	0.32		83.6
32	25	0.04	0.81	1.26			
22 22 53	+00 04 59	0.50	4.8	4.8	1.6		83.6
10	10	0.05	1.0	1.0			
22 33 47	−00 15 51	0.30	4.04	8.26	1.37	SNR	83.6
30	15	0.03	0.67	1.27			
22 44 1	−00 01 08	0.10	2.31	2.66	0.1		83.6
27	24	0.03	0.85	0.98			
22 45 59	−00 15 33	0.42	5.08	4.24	1.24		83.6
15	15	0.03	0.50	0.46			
22 45 52	−00 29 39	1.47	2.96	3.19	1.90	Compact H II	83.6
11	11	0.04	0.09	0.10			
22 51 12	−00 17 45	0.32	9.06	5.32	2.1		83.6
20	40	0.05	1.86	1.00			
22 56 9	−00 04 12	0.16	2.75	3.03	0.18		83.6
20	20	0.03	0.67	0.70			
23 6 39	+00 33 10	0.61	5.42	4.45	2.02	H II	83.6
11	12	0.02	0.27	0.24			
23 15 27	−00 17 17	0.77	4.49	6.31	2.99	H II	83.6
17	12	0.05	0.45	0.59			

Table 1. (Continued)

l / Δl	b / Δb	S_p / ΔS_p (Jy/beam)	θ_l / $\Delta\theta_l$	θ_b / $\Delta\theta_b$	S_t (Jy)	Remark	Date of observation†
23°16′13″	−00°27′25″	0.14	5′.74	5′.70	0.63	SNR	83.6
30	27	0.02	1.42	1.38			
23 22 2	+00 27 01	0.15	3.11	2.97	0.19		83.6
25	25	0.04	0.87	0.85			
23 25 34	−00 12 56	3.79	3.75	4.16	8.11	H II	83.6
11	11	0.10	0.12	0.14			
23 28 26	−00 18 43	0.50	4.2	4.2	1.21		83.6
14	14	0.05	1.0	1.0			
23 32 10	−00 02 24	0.94	4.56	4.20	2.47	H II	83.6
11	11	0.03	0.20	0.19			
23 37 43	−00 23 42	0.29	5.23	4.80	1.00		83.6
20	20	0.02	0.57	0.58			
23 40 30	+00 29 19	0.12	4.64	3.30	0.25		83.6
20	30	0.02	1.14	0.85			
23 42 57	−00 12 13	0.33	4.36	3.38	0.67		83.6
12	15	0.03	0.48	0.41			
23 42 32	+00 10 03	1.55	2.74	2.80	1.63	Compact H II	83.6
11	11	0.05	0.11	0.11			
23 44 34	−00 02 04	0.18	2.45	3.20	0.19		83.6
15	15	0.03	0.42	0.51			
23 49 49	+00 23 41	0.17	7.54	3.94	0.67		83.6
15	32	0.02	1.42	0.63			
23 48 57	+00 13 36	0.37	3.73	3.42	0.65		83.6
12	12	0.03	0.35	0.34			
23 50 6	+00 06 21	0.16	3.92	3.10	0.27		83.6
27	30	0.04	1.24	1.08			
23 52 26	−00 07 17	0.95	2.75	2.85	1.02	Compact H II	83.6
11	11	0.04	0.13	0.14			
23 55 48	−00 17 19	0.12	2.61	2.89	0.12		83.6
20	20	0.03	0.74	0.77			
23 57 28	+00 08 58	2.01	2.77	2.73	2.09	Compact H II	83.6
11	11	0.05	0.08	0.08			
23 59 44	−00 06 17	0.20	2.77	2.56	0.19		83.6
12	15	0.03	0.38	0.34			
24 7 40	+00 07 07	0.31	3.44	2.53	0.37		83.6
15	17	0.05	0.61	0.49			
24 8 51	+00 25 32	0.15	4.66	3.67	0.35		83.6
17	20	0.02	0.83	0.66			
24 11 44	+00 12 53	0.35	3.83	4.45	0.82		83.6
12	12	0.02	0.33	0.38			
24 12 39	−00 02 56	0.50	3.48	3.44	0.82	H II	83.6
12	15	0.05	0.39	0.37			
24 17 59	−00 09 28	0.45	4.81	3.99	1.18	H II	83.6
12	15	0.03	0.42	0.39			
24 23 38	+00 04 09	1.01	3.35	4.09	1.70	Compact H II	83.6
12	11	0.05	0.21	0.25			

Table 1. (Continued)

l Δl	b Δb	S_p ΔS_p (Jy/beam)	θ_l $\Delta\theta_l$	θ_b $\Delta\theta_b$	S_t (Jy)	Remark	Date of observation†
24°28′46″	+00°13′04″	1.16	6′.38	5′.63	5.72	H II	83.6
15	15	0.07	0.49	0.47			
24 28 8	+00 29 19	3.78	2.75	2.72	3.88	Compact H II	83.6
11	11	0.09	0.07	0.07			
24 30 20	−00 02 31	0.70	2.69	3.23	0.83		83.6
12	12	0.06	0.23	0.27			
24 31 24	−00 14 10	1.22	5.04	4.16	3.51	H II	83.6
12	12	0.05	0.31	0.27			
24 39 51	+00 35 35	0.26	4.84	5.15	0.89	SNR	83.6
17	17	0.03	0.71	0.75			
24 40 49	−00 09 28	1.77	2.91	3.47	2.45	Compact H II	83.6
12	11	0.10	0.19	0.23			
24 43 24	−00 42 51	0.12	4.02	5.63	0.37	SNR	83.6
32	25	0.03	1.19	1.68			
24 40 47	+00 05 50	2.60	3.97	4.19	5.93	H II	83.6
11	11	0.09	0.17	0.18			
24 55 36	+00 26 45	0.17	4.05	4.41	0.42		83.6
17	17	0.02	0.63	0.69			
24 57 51	−00 02 37	0.17	2.87	3.51	0.23		82.11
25	20	0.04	0.76	0.92			
25 16 8	−00 18 36	0.56	4.15	4.09	1.30	H II	82.11
11	11	0.02	0.21	0.21			
25 16 2	+00 18 33	0.47	3.17	3.65	0.75	Compact H II	82.11
12	12	0.03	0.25	0.28			
25 23 34	+00 33 53	0.27	3.86	3.08	0.44		83.3
15	17	0.03	0.51	0.46			
25 23 20	−00 10 12	7.86	3.37	4.61	18.54	H II	83.3
12	12	0.46	0.28	0.36			
25 23 52	+00 02 06	0.69	2.50	2.72	0.64	Compact H II	83.3
12	12	0.07	0.26	0.28			
25 23 25	−00 20 41	0.46	4.03	5.56	1.41		83.3
17	15	0.03	0.53	0.66			
25 31 39	+00 13 03	0.40	4.62	3.16	0.80		83.3
12	15	0.02	0.40	0.30			
25 42 3	+00 02 11	1.10	3.33	3.53	1.77	H II	83.3
11	11	0.06	0.20	0.21			
25 49 51	+00 00 13	0.22	4.78	2.18	0.31		83.3
12	25	0.03	0.83	0.40			

† Dates of observations are indicated as 82.11=November 1982, 83.3=March 1983, and 83.6=June 1983.

Column 3: Peak flux density at 10.05 GHz, S_p.
Column 4: Half maximum Gaussian width in the longitude direction, θ_l.
Column 5: Half maximum Gaussian width in the latitude direction, θ_b.
Column 6: Total flux density estimated through $S_t=S_p\theta_l\theta_b\theta^{-2}$ with θ (=2′.7) the HPBW of the antenna.
Column 7: Remarks.
Column 8: Date of observations.

Columns 1 through 5 give also the mean errors of each entry on the second line.

3.2. *A Comparison with the Bonn 5-GHz Survey*

A comparison of the results with the Bonn 5-GHz survey (Altenhoff et al. 1978) reveals many interesting features associated with the galactic structure and star forming regions. Because the HPBW of the both surveys are almost the same, the two data can be directly compared. We emphasize a good agreement in the general features found in the 10-GHz map with those found in the Bonn maps. However, a careful inspection of the two maps shows the following differences in appearances of the sources.

Sources with flat spectra with spectral indices $\alpha \gtrsim -0.3$ ($S \propto \nu^{\alpha}$ with the frequency ν), mostly thermal sources like H II regions, become more evident on the 10-GHz map compared with the 5-GHz maps. On the other hand, nonthermal sources with steep spectra become relatively fainter. To see this situation more clearly we superimpose the positions of the discrete sources detected in the Bonn survey in figure 2. Here the sources identified as compact H II regions (e.g., Downes et al. 1980) are indicated with filled squares, H II regions by circles, and the other sources with crosses and triangles. The crosses show the sources with $S_{5\mathrm{GHz}} \geq 0.2$ Jy and the triangles show the sources with $S_{5\mathrm{GHz}} < 0.2$ Jy and the sources with uncertain peak fluxes. It is impressive that many 5-GHz sources are hardly detected on the 10-GHz map with $S_{10\mathrm{GHz}} < 0.1$ Jy, which suggests their nonthermal origin. Indeed a determination of spectral indices for the sources with $S_{5\mathrm{GHz}} > 0.2$ Jy and $S_{10\mathrm{GHz}} > 0.1$ Jy shows that the majority of the weak sources have steep spectra of $\alpha \lesssim -0.5$. Figure 2 shows that thermal sources like H II regions are distributed well bound to the galactic plane, while the other weak sources are more diffusely distributed, although still concentrated toward the galactic plane.

3.3. *Background Emission*

The extended features in figure 1 are categorized into two types: discrete sources like SNRs and H II regions, and diffuse background emission. The background emission defines a band of radio enhancement $\sim 1^{\circ}$ wide running along the galactic plane. Hirabayashi (1974) has studied the spectrum of the background emission to discriminate thermal and nonthermal contributions in the frequency range from 1.4 GHz to 15 GHz. The surface brightness toward G25.07+0.01, where no significant sources are found as discussed in detail by Hirabayashi (1974), is estimated as $\sum = 6 \times 10^{-21}$ W m^{-2} Hz^{-1} sr^{-1} and agrees well with his spectrum. The spectrum is represented by a superposition of two components: the nonthermal component of $\alpha \approx -1$ and the thermal component of $\alpha \approx 0$. The spectrum shows that the thermal contribution at 10 GHz toward this direction is approximately 80% of the total emission.

3.4. *Supernova Remnants*

In the mapped area we find several SNRs which are catalogued by Milne (1979) and marked with dashed lines in figure 2.

SNR G21.5−0.9: This SNR appears as a compact source on the 10-GHz map with its total flux density $S_{10\mathrm{GHz}} = 4.7 \pm 0.1$ Jy. This source is known as a Crab-like SNR with a flat spectrum.

SNR G21.8−0.6: This SNR is composed of two arcs: a well defined, bright sourthern arc and a short northern arc with lower brightness. Such a double-arc appearance is often observed for shell-type SNRs and may be due to shock compression of magnetic fields running roughly parallel to the galactic plane.

SNR G22.7−0.2: This SNR is composed of a well-defined circular shell, particulary

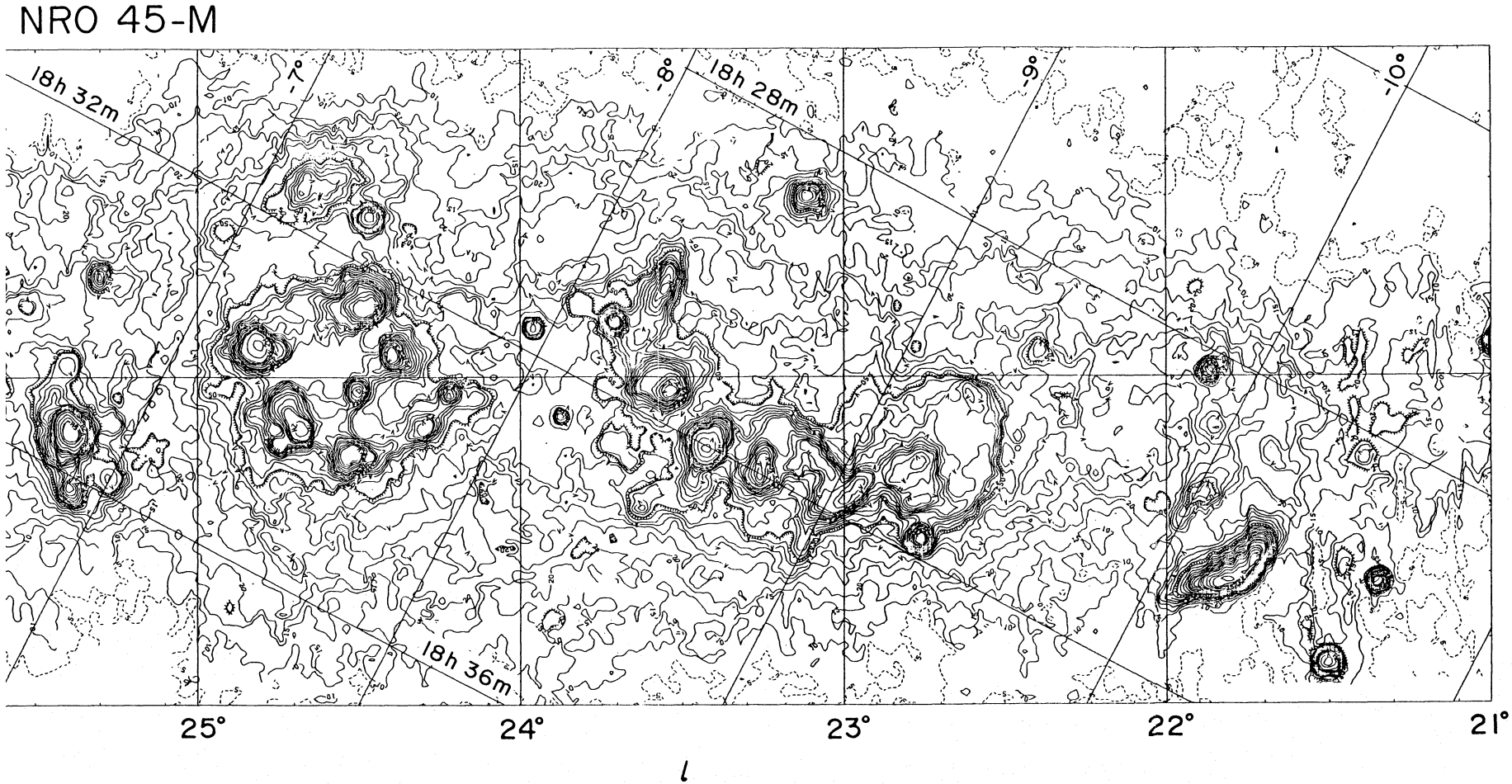

Fig. 1. The brightness distribution at 10.05 GHz of the galactic plane region at $l = 21 - 26$, $b = -1°$ to $+1°$. The unit of the numbers on contours is 21.8 mJy/beam area ($= 3.13 \cdot 10^{-25}$ W m^{-2} Hz^{-1} sr^{-1} $= 10.2$ mK in T_b). The HPBW is 2.7 and the rms noise on the figure is about 20 mK in T_b.

Hz, NRO 45-M

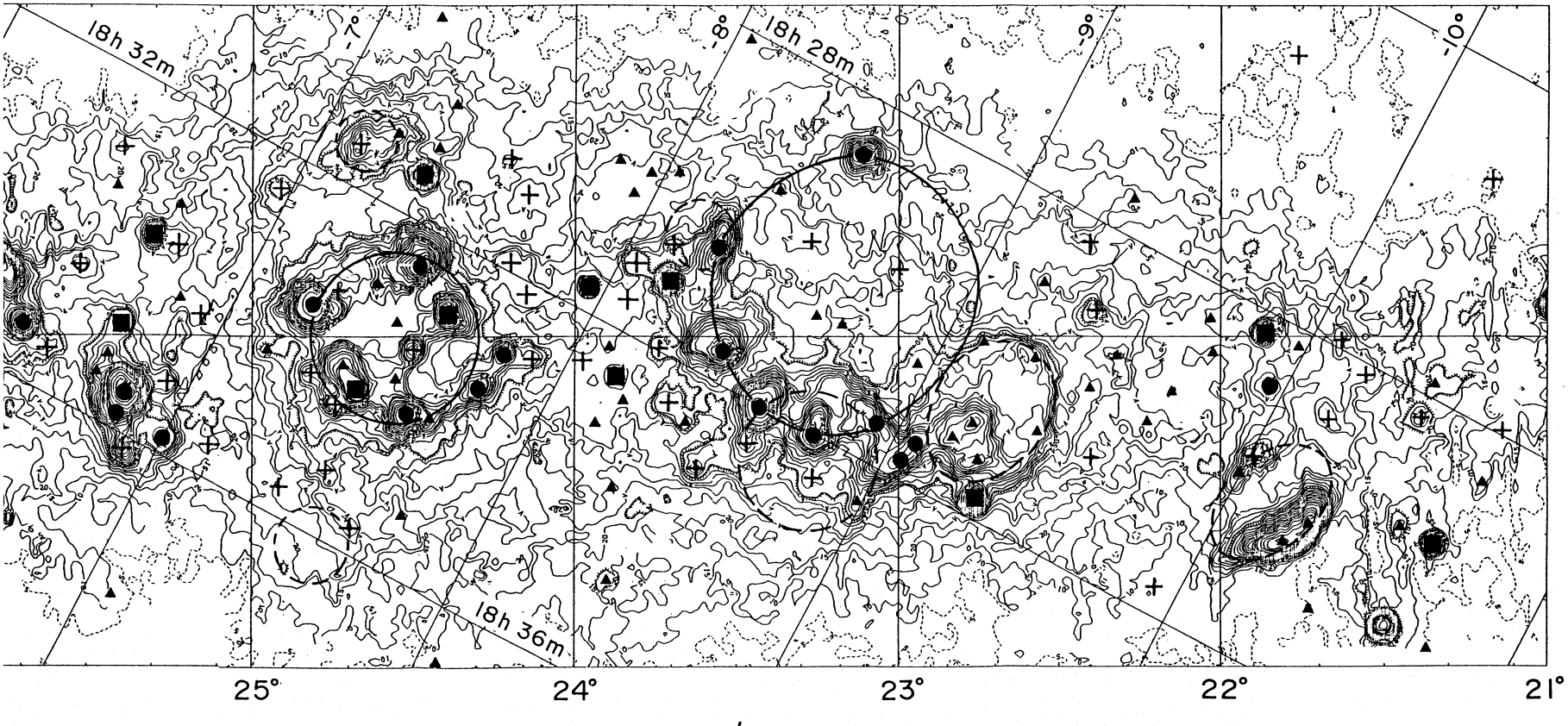

Fig. 2. Reproduction of figure 1, on which positions of 5-GHz radio sources from the Bonn survey are superimposed. Filled squares are compact H II regions, circles are H II regions, crosses are sources with $S_{5\mathrm{GHz}} > 0.2$ Jy, and triangles are sources with $S_{5\mathrm{GHz}} < 0.2$ Jy and uncertain peak fluxes. Two H II rings, G 24.6 + 0.0 and G 23.2 ± 0.2, are indicated with large circles. Catalogued SNRs are indicated with dashed lines.

on its western and southern parts.

SNR G23.3−0.3: This is composed of a few spurlike ridges and is superposed by a few H II regions which are part of the giant H II ring G23.2+0.2 (described later).

SNR G23.6+0.3: This is also superposed on the H II ring G23.2+0.2 and is not clearly seen in the present 10-GHz map because of the merging of the H II regions.

SNR G24.7−0.6: This appears on the 5-GHz Bonn map as an elongated spurlike ridge. On the 10-GHz map, however, this SNR appears only as a slight enhancement and does not show any defined structure, suggesting a very steep nonthermal spectrum.

SNR G24.7+0.6, a Crab-like SNR: This SNR has an irregular morphology with a filled center, and its peak flux spectrum between 10 and 5 GHz is as flat as $\alpha=-0.1$. In this respect this object seems to be a new candidate for a Crab-like SNR. In fact Reich et al. (1984) report a significant linear polarization at 5 GHz and confirm that this object is a Crab-like SNR.

3.5. *H II Rings*

The most interesting features found in figure 1 are ringlike associations of discrete sources. One ring appears as a circularly oriented H II regions, mostly compact, centered on $l=24\overset{\circ}{.}6$, $b=0°$ with its diameter of about 40′. This ring complex is composed of several H II regions embedded in an extended envelope of radio emission: the H II regions are connected with diffuse bridges of radio emission. In fact, if we remove discrete sources which can be fitted with Gaussian distributions, there remains a plateaulike round distribution of radio emission with a diameter ∼40′. We hereafter refer to this complex as "H II ring G24.6+0.0" after its center position. Radial velocities of the H II regions range from 100 to 115 km s^{-1} (Downes et al. 1980; Wink et al. 1982). If we adopt a kinematical distance of 9 kpc for the ring, the diameter is about 80 pc.

Another ring is found as a large association aligned along an arc extending from $(l, b)=(22\overset{\circ}{.}8, -0\overset{\circ}{.}2)$ to $(23\overset{\circ}{.}7, +0\overset{\circ}{.}2)$. The center of the arc when fitted to a circle of diameter 50′ is at $l=23\overset{\circ}{.}2$, $b=0\overset{\circ}{.}3$. This arc is composed of a mixture of H II regions and supernova remnants. We may call this complex H II ring G23.2+0.3. The radial velocities of the H II regions are from 80 to 100 km s^{-1}. If the kinematical distance is adopted to be 7 kpc, the linear diameter of the ring is about 100 pc. An H II region at G23.1+0.6 may be also associated with this ring, although its radial velocity is unknown.

The origin of the rings is not clear as yet. However, we may recall that a ring of H II regions in the anticenter direction, called the Origem Loop, has been noticed by Berkhuijsen (1974), whose diameter is about 60 pc. The loop is thought to be a shock enhanced star formation region by an old supernova remnant. The diameters of G24.6+0.0 and G23.2+0.2 are comparable to that of the Origem Loop. However, the H II regions in the two rings are more intense than those found on the Origem Loop.

3.6. *Weak Nonthermal Sources*

A large number of weak radio sources have steep spectra, suggesting their nonthermal nature. Their origin and physical properties remain uncertain. From their concentration towards the galactic plane they are galactic sources. We discuss below some possible origins of the sources.

(*a*) *Small-size, low-brightness SNR*

If the sources are normal SNRs we can estimate the diameter and distance using a surface brightness–diameter relation (e.g., Clark and Caswell 1976; Milne 1979). If we take a typical flux density of ∼0.4 Jy at 5 GHz for the sources and source sizes of ∼2′,

we have surface brightness at 5 GHz of $\sim 10^{-20}$ W m^{-2} Hz^{-1} sr^{-1}. Applying the surface brightness–diameter relation of Clark and Caswell (1976), we obtain a distance of ~ 50 kpc and a diameter of ~ 30 pc. The distance is in contradiction to the fact that they are galactic sources, and we may conclude that they are not normal SNRs.

(*b*) *Very rapid pulsars*

A considerable fraction of the weak sources are compact (table 1). Some of the sources might be very rapid pulsars which have stronger radio emission and much shorter period than those so far discovered. The short period may make it difficult to detect them as pulsars, and the large dispersion measure at low galactic latitudes will make the situation worse.

(*c*) *Background fluctuations*

Because of the nonthermal nature we finally consider a possible origin of the weak sources as small-scale condensations of magnetic fields and cosmic rays in the interstellar medium. Such condensations may be produced by interstellar turbulent motions such as those due to supernova explosions. Fragments of unidentified old SNR shells could also be seen as such local condensations. If the distances are 1–10 kpc, their sizes are of the order of 1–6 pc. Then their luminosity at 1–10 GHz is roughly of the order of 10^{31} erg s^{-1}. If we assume an equilibrium between the magnetic energy and cosmic ray energy densities in the source, we have a magnetic field strength of 30 μG. This strength is only an order of magnitude greater than the strength of the mean interstellar magnetic field.

4. Concluding Remarks

The radio continuum survey at 10 GHz of the galactic plane region provides an important clue to clarify the thermal and nonthermal contributions to the background radio emission which has a transient frequency at around 5–10 GHz. The 10-GHz survey may give also a powerful means to discriminate thermal (or flat spectrum) sources from nonthermal sources when compared with a lower frequency survey data of a comparable angular resolution.

The importance of the 10-GHz survey has been confirmed by the discovery of several interesting objects through a comparison with the Bonn 5-GHz survey. One of the remarkable objects is the Crab-like SNR G24.6+0.7 with filled center morphology and a flat spectrum. Other interesting objects are the two H II rings G24.6+0.0 and G23.2+0.2, which are circular orientations of H II regions with diameters of about 100 pc embedded in diffuse radio emitting regions. A number of less intense sources are shown to be nonthermal. Such weak nonthermal objects distributed near the galactic plane have never attracted the astronomers' interest. Although we have given some possible origins, the pulsar origin hypothesis for very compact sources seems attractive. In fact, a statistical estimation of the total number density of pulsars in the Galaxy is $\sim 10^2$ pulsars kpc^{-2} at galactocentric distances 4–10 kpc confined within a disk of thickness 0.4 kpc (Lyne 1982). This means that we may see more than a few hundred pulsars in the field in figure 1. It is therefore likely that the strongest pulsars of very short period among them are observed as compact nonthermal radio sources in the presently mapped area.

The authors acknowledge the staff of NRO for the help in the observations. One of the authors (Y.S.) is indebted to the A. von Humboldt-Stiftung for the fellowship from

June through September 1983, which allowed him to stay at the Max-Planck-Institut für Radioastronomie in Bonn. He is also indebted to Professor R. Wielebinski for the discussion and hospitality.

References

Altenhoff, W. J., Downes, D., Pauls, T., and Schraml, J. 1978, *Astron. Astrophys. Suppl.*, **35**, 23.
Baars, J. W. M., Genzel, R., Pauliny-Toth, I. I. K., and Witzel, A. 1977, *Astron. Astrophys.*, **61**, 99.
Berkhuijsen, E. M. 1974, *Astron. Astrophys.*, **35**, 429.
Clark, D. H., and Caswell, J. L. 1976, *Monthly Notices Roy. Astron. Soc.*, **174**, 267.
Downes, D., Wilson, T. L., Bieging, J., and Wink, J. 1980, *Astron. Astrophys. Suppl.*, **40**, 379.
Haslam, C. G. T. 1974, *Astron. Astrophys. Suppl.*, **15**, 333.
Hirabayashi, H. 1974, *Publ. Astron. Soc. Japan*, **26**, 263.
Lyne, A. G. 1982, in *Supernovae: A Survey of Current Research*, ed. M. J. Rees and R. J. Stoneham (D. Reidel Publishing Co., Dordrecht), p. 405.
Milne, D. K. 1979, *Australian J. Phys.*, **32**, 83.
Reich, W., Fürst, E., and Sofue, Y. 1984, *Astron. Astrophys.*, **133**, L4.
Sofue, Y., Hirabayashi, H., Akabane, K., Inoue, M., Handa, T., and Nakai, N. 1983, in *The Milky Way Galaxy, IAU Symp. No. 106*, ed. H. van Woerden (D. Reidel Publ. Co., Dordrecht), in press.
Sofue, Y., and Reich, W. 1979, *Astron. Astrophys. Suppl.*, **38**, 251.
Tabara, H., Kato, T., Inoue, M., Aizu, K. 1984, *Publ. Astron. Soc. Japan*, **36**, 297.
Wink, J. E., Altenhoff, W. J., and Mezger, P. G. 1982, *Astron. Astrophys.*, **108**, 227.